

Regenerative response of rat skeletal muscle to the implantation of a collagen-based bone graft substitute: an *in vivo* study

Fernando Leiva-Cepas,^{1,2,3*} Maria Jesus Gil-Belmonte,^{1,4*} Ignacio Jimena,^{1,2} Maria Angeles Peña-Toledo,^{1,2,5} Rafael Villalba,^{2,6} Jose Peña-Amaro^{1,2}

¹Research Group in Muscle Regeneration, Department of Morphological and Sociosanitary Sciences, Faculty of Medicine and Nursing, University of Cordoba, Cordoba, Spain; ²Maimonides Institute for Biomedical Research IMBIC, Reina Sofia University Hospital, University of Cordoba, Spain; ³Department of Pathology, Reina Sofia University Hospital, Cordoba, Spain; ⁴Department of Pathology, Torrecardenas University Hospital, Almeria, Spain; ⁵Dementia and Multiple Sclerosis Unit, Neurology Service, Reina Sofia University Hospital, Cordoba, Spain; ⁶Tissue of Establishment of the Center for Transfusion, Tissues and Cells, Cordoba, Spain.

*These authors contributed equally to this work.

This article is distributed under the terms of the Creative Commons Attribution Noncommercial License (CC BY-NC 4.0) which permits any noncommercial use, distribution, and reproduction in any medium, provided the original author(s) and source are credited.

Abstract

The application of implantable biomaterials in reconstructive grafting is a common practice in surgical fields such as orthopedics, maxillary and plastic surgery. This study explores the regenerative response of skeletal muscle to a porous bovine collagen-based matrix (Osteovit®) in a volumetric muscle loss injury model. Forty male Wistar rats were divided into four groups. Normal control underwent no procedure and regenerative control had mepivacaine injected in the tibialis anterior muscle to provoke a standard regenerative response. In the other two groups, a volumetric defect was created in the tibialis anterior muscle; the fibrosis control had no treatment, while the collagen-scaffolding group had a bone substitution matrix implanted. Animals were sacrificed at 21, 28, and 60 days post-procedure for histological, histochemical, immunohistochemical and histomorphometry analysis to evaluate muscle architecture and myogenic regenerative response. Significant changes in tissue architecture among groups, with a notable emphasis on the integration of the collagen scaffold, were demonstrated. This was also confirmed at the histomorphometry analysis, which found differences at the cross-sectional area, minor diameter and form factor values between groups. The bone substitution matrix did not inhibit regeneration but promoted an abnormal one. This can be explained by the excessive formation of connective tissue, which led to the genesis of intramuscular tendons that may have interfered with the normal development of regenerative muscle fibers. The findings highlight the need for further investigation into the cellular mechanisms underlying skeletal muscle regeneration in response to implantable biomaterials.

Key Words: skeletal muscle, muscle regeneration, volumetric muscle loss, collagen matrix scaffold, bone substitute, fibrosis.

Eur J Transl Myol 35 (4) 13574, 2025 doi: 10.4081/ejtm.2025.13574

Skeletal muscle is well known for its high regenerative capacity in response to injury, primarily owing to the presence of myogenic progenitor cells, the satellite cells.^{1,2} While there are some differences based on the type and extent of the injury, the process of skeletal muscle tissue damage and regeneration comprises a general sequence of three overlapping stages: i) the destruction and inflammation phase, ii) the regenerative phase, characterized by the activation, differentiation, and fusion of satellite cells, and iii) the maturation and remodeling phase of the regenerated muscle.^{3,4}

The use of implantable biomaterials for reconstructive grafting procedures is a standard technique utilized across various surgical disciplines, such as orthopedics, plastic surgery, and maxillofacial surgery, aimed at repairing tissue or organ defects.⁵ Understanding the tissue response to these implants, with special attention to the degree of histoarchitectural integration, is of significant interest in the field of regenerative medicine within these areas. In major injuries or traumas, both bones and muscles can be affected simultaneously.⁶ Because of this, the use of implant materials in bone reconstruction can affect

the regenerative capacity of adjacent injured muscles. Notably, skeletal muscle has been reported to exhibit host versus graft reactions, muscle atrophy, and an increase in the slow myosin isoform following the intramuscular implantation of bone substitution materials.⁷ However, considering the great regenerative capacity of skeletal muscle, it is surprising that no documentation has been provided on how the regenerative response of muscle fibers may be affected by the implantation of this type of material.

In the present study, we examine the regenerative response of skeletal muscle after the implantation of a porous collagen type I (spongiosa) matrix of bovine origin devoid of any antigenic element (Osteovit[®]) in a volumetric muscle loss injury model. This material has been successfully applied in orthopedic procedures to fill bone defects.⁸ In a previous study, we assessed the integration of this material into skeletal muscle using ultrasound, encountering that both echogenicity and echotexture were significantly altered.⁹ However, to date, we had not addressed the histological substrate that explains this ultrasound pattern.

Material and Methods

Animals

All experiments were performed using male Wistar rats weighing approximately 300 g. Animals were maintained in cages at 22°C under a 12-h light/12-h dark cycle and were allowed free access to food. All experimental procedures were conducted following Directive 2010/63/EU of the European Council and Parliament governing the protection and use of animals for scientific purposes. The study was approved by the General Directorate of Agricultural and Livestock Production of the Junta de Andalucía (Ref. 07/09/2017/121), the Ethics Committee for Animal Experimentation at the University of Cordoba (Ref. 2017IP/05).

Experimental procedures

A previously fixed sample cohort of forty male Wistar rats (n=40), weighing 350±50g (mean±SD) was divided into four groups: i) Normal Control (NC), formed by rats (n=4) that were not subjected to any manipulation; ii) Regenerative Control (RC), formed by rats (n=12) that were injected intramuscularly into the tibialis anterior muscles with 100 µl of mepivacaine hydrochloride 2% (Scandinibsa[®]; Inibsa, Barcelona, Spain), a local anesthetic that generates a myotoxic injury followed by a rapid and complete regenerative response in skeletal muscle.¹⁰ The injection was performed with a fine needle that was introduced, from the distal region to the proximal region, through the central portion of the muscle, releasing the myotoxic as the needle was withdrawn; iii) Fibrosis Control (FC) formed by rats (n=12) that were only treated with an absorbable hemostatic sponge (Gelita-Spon standard[®], Gelita-Medical[®], Eberbach, Germany) after a volumetric defect created in the tibialis anterior muscle; (iv) Collagen Scaffold (CS) formed by rats (n=12) that were implanted

with a resorbable bovine collagen matrix (Osteovit[®], Braun, Spain) in a volumetric defect created in the tibialis anterior muscle (*Supplementary Figure 1*).

To induce the volumetric defect in the FC and CS groups, the procedure described in previous publications was followed.^{9,11} Briefly, the tibialis anterior muscles were exposed, and a sterile punch (6 mm in diameter and 5 mm in length) was used to perform a biopsy, removing a cylindrical fragment of tissue from the central portion of the muscle belly and creating a cavity (*Supplementary Figure 1*). During the procedure, a tourniquet was applied for 3–4 minutes proximal to the excision site to reduce bleeding. The wound site was then closed with surgical staples and cleaned. Animals were given appropriate postoperatively analgesia and antibiotic prophylaxis during the next three days following the procedure. In RC, FC and CS groups, animals were sacrificed after 21, 28 and 60 days of evolution (4 rats each time). Rats from the NC group were sacrificed after 60 days.

Histological analysis

Muscles were frozen in liquid nitrogen-cooled isopentane (2-methylbutane; Sigma-Aldrich, St. Louis, MO, USA) and then cut transversely into 8 µm cryosections on a cryostat (Leica CM1850 UV, Leica Microsystems, Nussloch, Germany).

The muscle sections were stained with histological, histochemical, and immunohistochemical techniques using standard methodology.¹² Haematoxylin and Eosin (H&E) staining was used for morphological analysis of skeletal muscle fibers, and Masson's trichrome stain was used to examine connective tissue and fibrosis. With Herovici's polychrome staining, we differentiated between type I collagen (red-purple staining), and type III collagen (blue staining), which can be used to study the remodelling response of the extracellular matrix. We used the Nicotinamide dinucleotide tetrazolium reductase (NADH-tr) histochemical technique to identify muscle fiber types and cytoarchitectural changes. We also studied immunohistochemical reactions with desmin (1:100, clone D33, Dako[®]) to identify regenerating muscle fibers and cytoarchitectural changes and MyoD1 (1:50, clone 58A, Dako[®]) to identify myogenic response.

Histomorphometric analysis

Samples corresponding to 60 days of evolution were photographed using a Nikon Eclipse E1000 microscope (Nikon, Tokyo, Japan) incorporating a Sony DXC-990P color video camera (Sony, Tokyo, Japan). Five fields (20x magnification) representative of the injured area were evaluated for each muscle. The images obtained for the morphometric analysis were then transferred to a computer and analyzed using Image J2 Fiji software (National Institutes of Health, Bethesda, MD, USA)¹³ for measurement of fibrosis area (%) and the following morphometry parameters of skeletal muscle fibers: cross-sectional area (µm²), minor diameter (µm), and form factor or circularity (0 through 1). Form factor is a shape descriptor that ranges from 0 to 1 and establish how similar a particle is to a cir-

cle. Any particle scoring «0» would be considered to have an extremely irregular shape, and the value «1» would represent a perfect circle). Color thresholding was performed on the Herovici's polychrome-stained samples to identify areas corresponding to collagen types I and III within the image. The results are expressed as a percentage calculated from the total of connective tissue.¹⁴ The number of cytoarchitectural changes (fibers with internalized nuclei, split fibers, ring fibers, and whorled fibers) was evaluated semiquantitatively in H&E, NADHtr, or anti-desmin stained sections under a light microscope. Each parameter was assigned a score 1 through 4 per microscopic field (100), whereby grade 1 (<25%), grade 2 (26–50%), grade 3 (51–75%), and grade 4 (>76%).

Statistical analysis

Data is presented as mean±standard error of the mean (SEM) for the total of areas evaluated for every histomorphometry parameter at each sample (cross-sectional area, minor diameter, form factor and fibrosis). We conducted a one-way ANOVA analysis of variance followed by the Scheffé or the Games-Howell *post-hoc* test. For non-normally distributed data, we performed a Kruskal-Wallis test followed by Mann Whitney-U pairwise comparison. The analysis of morphometric parameters was carried out using the SPSS 25® statistical software package. We defined significance as $p<0.05$.

Results

Perimysial septa separate the muscle fibers belonging to the NC group into well-delimited fascicles. These fibers displayed a polygonal morphology, have acidophilic sarcoplasm, and possess peripheral nuclei. No signs of necrosis or regeneration are observed. Normal muscle fibers lack immunostaining for MyoD1 and desmin.

21 days

The muscles in the RC group displayed numerous fibers with internalized nuclei and splitting muscle fibers, identifiable by their distinct profiles and invaginations. In contrast, the volumetric defect in the FC group was filled with abundant fibro-adipose tissue, where a few small, isolated regenerating muscle fibers could be seen near the edges of the lesion.

In the CS group, the implantation area was occupied by fibro-adipose tissue, and there was an inflammatory reaction surrounding the implanted material. Additionally, regenerating muscle fibers of uneven sizes and blood vessels were present within the porous spaces of the implant. The regenerating fibers displayed different intensities of desmin staining and contained numerous MyoD1+ nuclei (Figure 1).

28 days

Muscle samples from the RC group had regenerative muscle fibers showing some variability in size and central and internalized nuclei. No fibrosis foci were identified. The

absence of MyoD1+ nuclei was constated, and only a few muscle fibers strongly stained for desmin were occasionally observed. Remarkably, in the FC group, there was an area of fibrosis surrounded by small atrophic muscle fibers bordering the edge of the lesion.

In the CS group, scattered rests of the implanted material exhibiting a basophilic stain were identified surrounded by fibro-adipose tissue as well as by regenerating muscle fibers of variable size with internalized nuclei (Figure 2). Notably, within the dense fibrous tissue, certain areas exhibited a distinctly parallel orientation of both collagen fibers and nuclei (Figure 2). The number of MyoD1+ nuclei and desmin+ muscle fibers was reduced.

60 days

The muscles belonging to the RC group showed muscle fibers of polygonal or rounded morphology with internalized nuclei and muscle fibers of variable size with complementary profiles suggestive of splitting fibers. The muscles of the FC group were characterized by the presence of a wide area of fibrosis with scattered small muscle fibers. No changes or abnormal features were observed with the NADH-tr and desmin antibody staining techniques.

All samples from the CS group contained large intramuscular tendons at the implantation area (Figure 3). The surrounding muscle fibers exhibited two different histological patterns: i) adjacent zones with significant atrophy, together with marked endomysial and perimysial fibrosis and absence of differentiation of muscle fiber types (*Supplementary Figure 2*); and ii) areas with regenerated muscle fibers of different sizes with internalized nuclei and inadequate fiber-type differentiation, but with important abnormalities in their morphology and cytoarchitecture such as spiral fibers and ring fibers (Figure 4). Semi-quantitative analysis showed that cytoarchitectural abnormalities in muscle fibers were more evident in the CS group (Table 1).

Morphometric analysis revealed significant differences ($p<0.05$) in the muscle fibers size of the NC group (Figure 5a) concerning the groups FC and CS, which represented a decrement of 79,5% ($p<0.05$) and 52% ($p<0.05$) in the fiber cross-sectional area, respectively. The RC group scored significantly higher in the cross-sectional area than the FC and CS groups (Table 2). Values obtained for minor diameter (Figure 5b) followed a similar pattern to that observed in the cross-sectional area (Table 2). The shape descriptor labelled as form factor (Figure 5c) had significantly higher values in the NC group than in the CS group, constituting a 29% ($p<0.05$) decrease in the circularity of myofibers (Table 2). No statistically significant differences were found between the NC and the RC groups nor between the FC and CS groups at any parameter (Figure 5 a-c) (Table 2).

The percentage of connective tissue per field was also quantified, and a significant increment of 13% ($p<0.05$) was observed between the NC and the CS groups. FC group scored the highest fibrosis and differed significantly in this parameter compared to the CS group, which showed a 52% decrease ($p<0.05$) in the amount of con-

Regenerative response of rat skeletal muscle to the implantation of a collagen-based bone graft substitute

Eur J Transl Myol 35 (4) 13574, 2025 doi: 10.4081/ejtm.2025.13574

nective tissue (Figure 5d). Image analysis of the sections stained with Herovici's polychrome revealed differences in the percentages of collagen types I and III in the different groups (*Supplementary Figure 3*): NC (6.6% vs 48.9%), CR (47.5% vs 52.5%), FC (80.3% vs 4.3%), and CS (78.5 vs 11.9%).

Discussion

Our study demonstrated that the implanted matrix integrated well into the lesion. It did not cause any capsular reaction or hinder the regenerative response, which began at the edges of the injury. This is confirmed by the presence of myogenic markers -MyoD1, and desmin- observed on days 21 and 28. In contrast, there was virtually no positive staining for these markers in the RC group at that time. Given the injury mechanism, regeneration in the RC group was already completed by day 20.¹⁰ This difference can be attributed to a prolonged degenerative-regenerative process in the setting of a volumetric mass loss.¹⁵ Based on our results, we believe that the muscle atrophy that occurs after the application of bone replacement ma-

terial to skeletal muscle⁷ is a consequence of atrophy of regenerative muscle fibers.

The myogenic response, progressing from the preserved borders towards the implant, may be positively influenced by matrix collagen type I composition. While some studies have demonstrated that collagen scaffolding or similar biomaterials can enhance skeletal muscle regeneration in volumetric lesions,^{16,17} other research presents opposing views.¹⁸ Various investigations indicate that untreated volumetric defects are filled with fibrotic scarring tissue rich in collagen type I, leading to a defective regenerative response.¹⁹ This observation aligns with our findings in the FC group, where the fibrosis rate reached 75%. Since the CS group only scored 36% for fibrosis, it is evident that muscle regeneration was not impeded. However, the Herovici's polychrome staining demonstrated that the proportion of collagen type I was similar for the FC (80.3%) and CS (78.5%) groups, differing from the RC group (47.5%). Studies on fibrosis in dystrophic muscle have reported that the production of collagen type I inhibits regeneration while promoting additional collagen synthesis.²⁰ Furthermore, the absence of other components

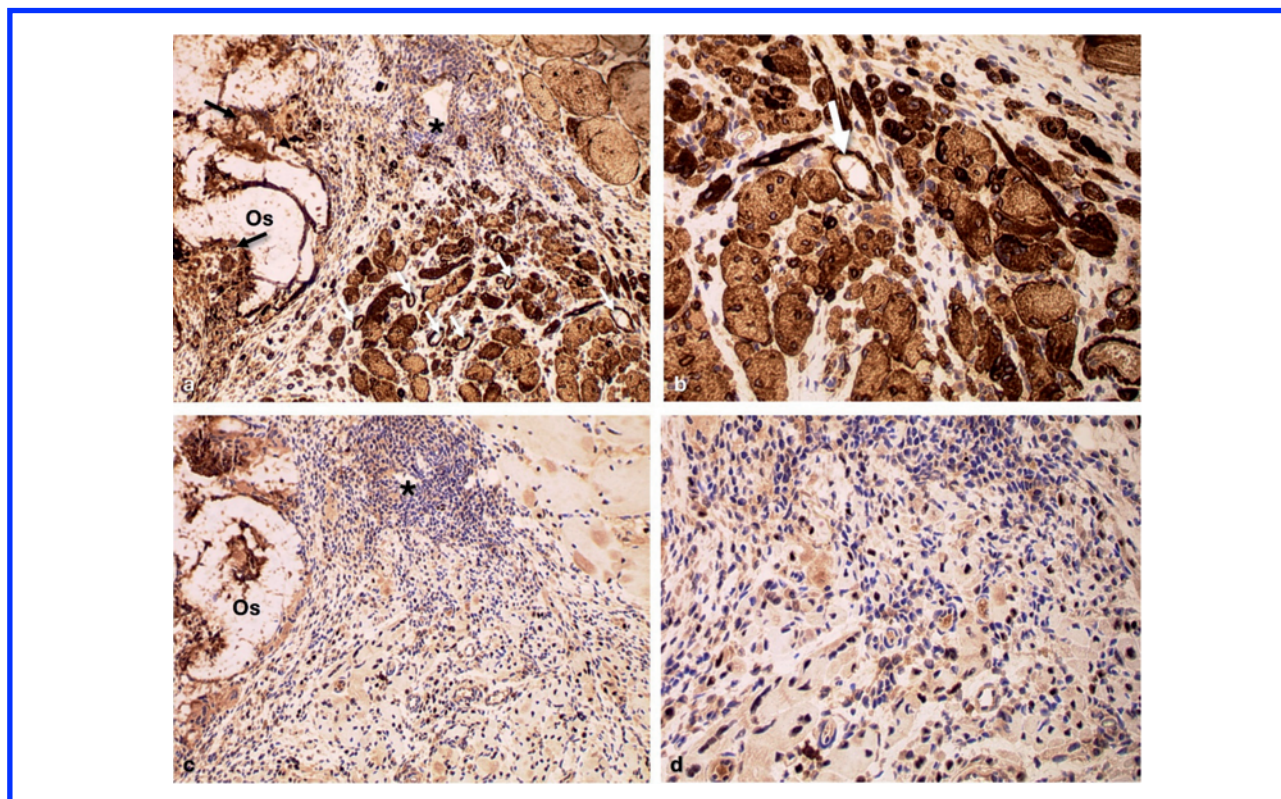


Figure 1. CS group. Twenty-one days postimplantation. (a) Regenerating muscle fibers of variable size and blood vessels (white arrows) on the right, unstained collagen implant on the left (Os). A prominent inflammatory infiltrate separates both elements. Black arrows indicate inflammatory and mononucleated desmin+ cells entering the implant. (b) Detail of image (a) showing desmin+ muscle fibers of different sizes with internalized nuclei and small mononucleated cells intensely stained with desmin. The white arrow points to a vascular lumen. Original magnification: a, 20x; b, 40x. (c) Collagen implant (Os) with a prominent inflammatory infiltrate (asterisk) and abundant MyoD1+ nuclei. (d) Detail of image (c) showing MyoD1+ nuclei of regenerating muscle fibers and mononucleated cells. Original magnification: a, c 20x; b, d 40x. a, b Anti-desmin; c, d Anti-MyoD1.

Regenerative response of rat skeletal muscle to the implantation of a collagen-based bone graft substitute

Eur J Transl Myol 35 (4) 13574, 2025 doi: 10.4081/ejtm.2025.13574

in this matrix may restrain the development of the myogenic response. For instance, *in vitro* studies have shown that modified type I collagen films with a combination of Matrigel and laminin/entactin significantly enhance myotube formation.²¹

Given that the bone matrix implanted in our study is exclusively made of type I collagen, the uninhibited regeneration could be justified, in our opinion, by its porous nature, which may have facilitated the growth of regenerating muscle fibers and blood vessels inwards from the periphery.^{22,23} However, cytoarchitectural abnormalities in the regenerated muscle fibers and significant areas with fascicular atrophy indicate that the growth and development of the regenerating muscle fibers were negatively

affected. The absence of alignment on the inside of the scaffold may have contributed to this abnormal regenerative response.²⁴

Central or internalized nuclei are frequently observed in regenerated muscle fibers.^{25,26} Nevertheless, additional cytoarchitectural abnormalities such as ring fibers and whorled fibers, as well as other of an irregular morphology (as demonstrated by form factor shape descriptor), are associated with impaired maturation. This phenomenon is attributed to the development of muscle fibers in an adverse tissue environment.^{11,27,28} Notably, collagen III constituted 52.5% of the composition in the RC group, whereas it comprised only 11.9% in the CS group. Given that collagen III plays a crucial role in providing elasticity

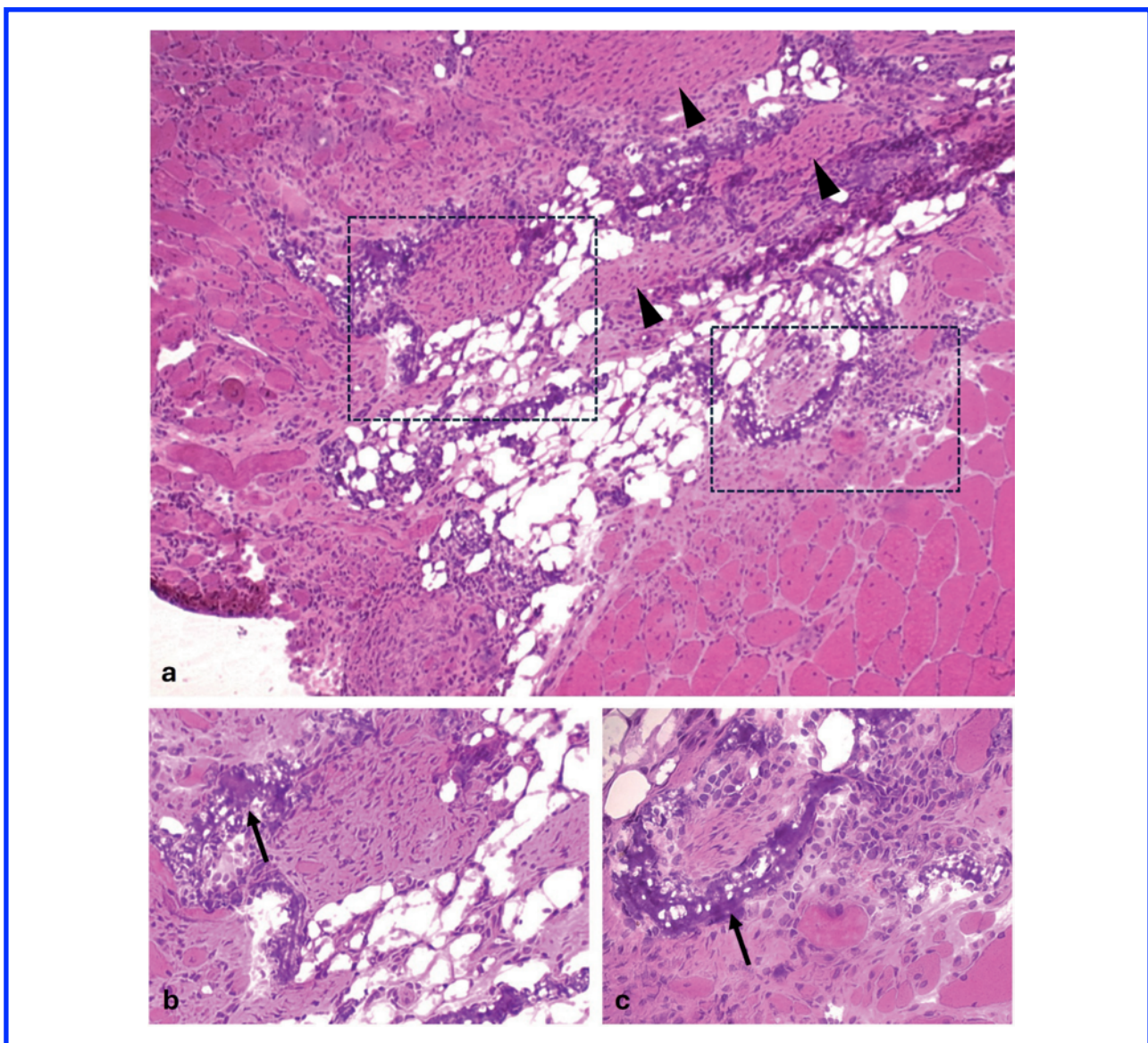


Figure 2. CS group. Twenty-eight days postimplantation. (a) The collagen matrix rests appear as irregular basophilic fragments in the proximity of inflammatory cells, adipocytes, and areas of connective tissue with a certain degree of orientation (arrowhead). (b) and (c) Insets of image (a) Regenerating muscle fibers of variable size and internalized nuclei surrounding the remaining fragments of the implanted material. Original magnification: a, 10x; b, 20x; c, 40x. H&E.

Regenerative response of rat skeletal muscle to the implantation of a collagen-based bone graft substitute

Eur J Transl Myol 35 (4) 13574, 2025 doi: 10.4081/ejtm.2025.13574

to the endomysium and perimysium,²⁹ the diminished levels in the CS group may have hindered the remodeling of the extracellular matrix during the regeneration process. Consequently, this lack of collagen may have adversely affected the growth and development of regenerating muscle fibers. This has led to the regeneration of morphologically abnormal fibers and the atrophy of others due to difficulties in their innervation. The excessive development of connective tissue during regeneration stops regenerative muscle fibers' reinnervation by creating

physical barriers hindering nerve fibers' growth.³⁰ In the present study, a significant fascicular atrophy with marked perimysial septa is indicative of a failure in the innervation of regenerating muscle fibers, similar to that which occurs in some neurogenic processes in human neuromuscular pathology.³¹ All this explains the ultrasound pattern described in a previous study.⁹ Along with the regenerative response of skeletal muscle to the implantation of the osteogenic matrix, large intramuscular tendons were also seen in the samples of the CS

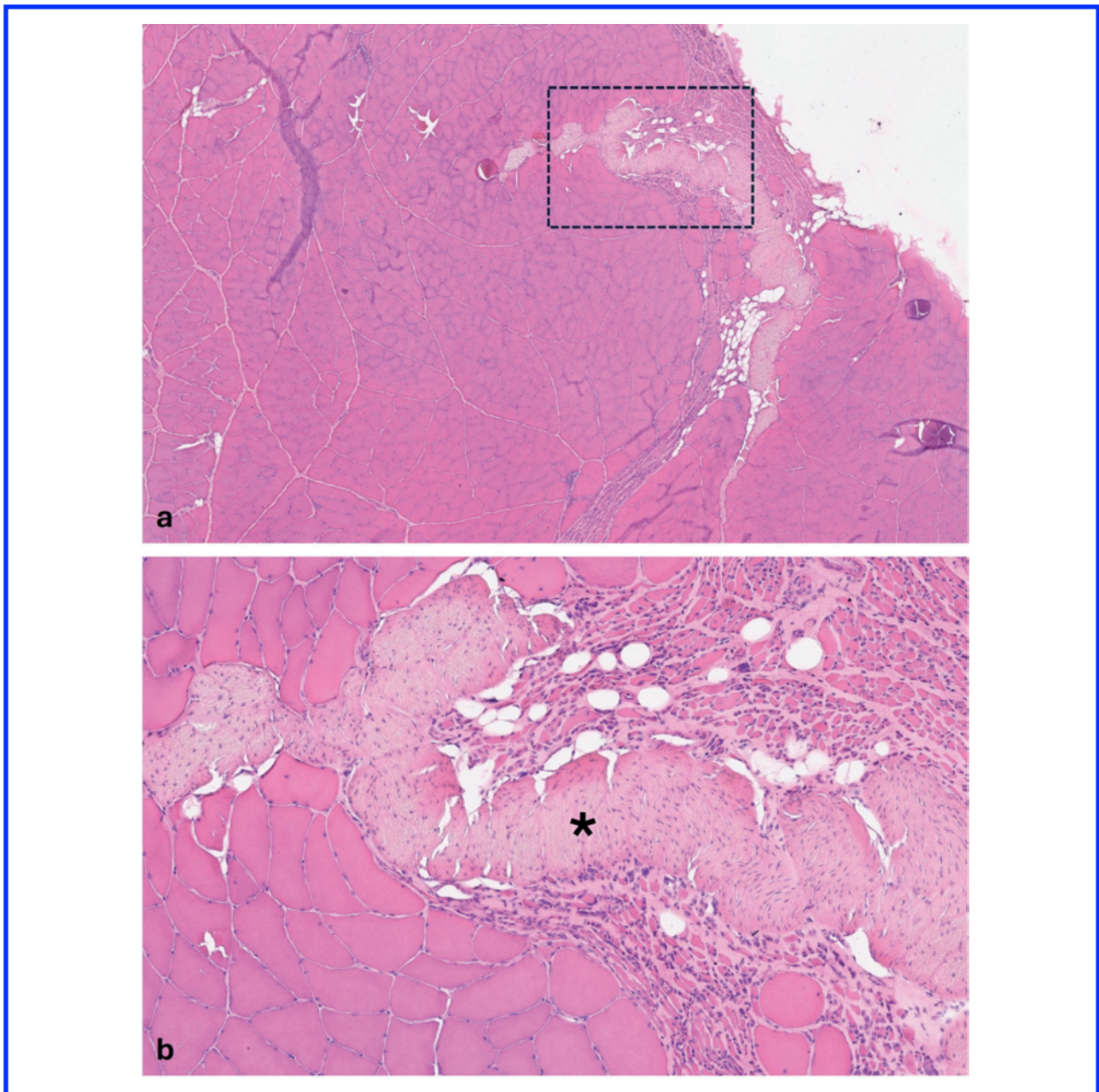


Figure 3. CS group. Sixty days postimplantation. (a) Panoramic image showing a pale-colored intramuscular tendon near the surface of the muscle. (b) Inset of image (a). The asterisk marks the tendon surrounded by an extremely fascicle of extremely atrophic muscle fibers with notable endomysial and perimysial fibrosis, including adipocytes. Original magnification: a, 5x; b, 20x. H&E.

Regenerative response of rat skeletal muscle to the implantation of a collagen-based bone graft substitute

Eur J Transl Myol 35 (4) 13574, 2025 doi: 10.4081/ejtm.2025.13574

group but not in the rest of the groups at 60 days. According to our observations, after 28 days of implantation, an apparent arrangement in the orientation of fibrotic areas takes place. This connective tissue rearrangement may involve an underlying process of tendon neoformation out of the implanted matrix. Therefore, we think that the matrix used in our study could be of interest in the research of the reconstruction of injured tendons in which collagen compounds are used³² as well as for the study of the generation of new myotendinous junctions.

On the other hand, since Osteovit[®] is an osteogenic material, intramuscular ossification could have occurred, especially considering the type of injury caused in which significant regeneration and repair happened. Heterotopic ossification in skeletal muscle is a problem of great interest in sports traumatology. Likely, it is the result of an alteration of the biochemical or environmental signals in the balance of skeletal muscle regeneration.³³ Although this is a different situation from our experimental approach, which combines a muscle injury and osteogenic matrix

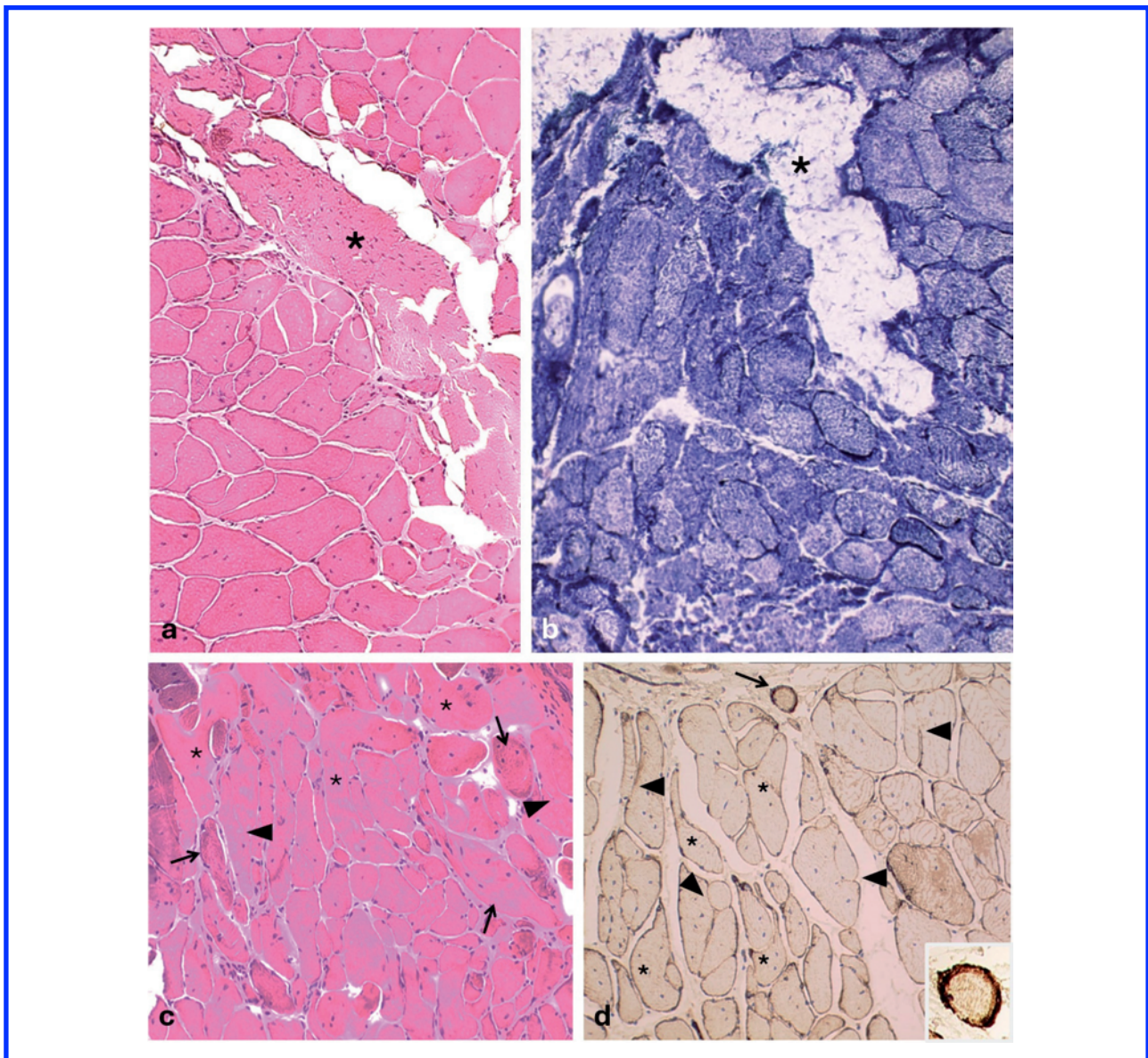


Figure 4. CS group 60 days postimplantation. (a) The asterisk marks a tendon surrounded by muscle fibers of different sizes, irregular morphology, and internalized nuclei. (b) The intramuscular tendon (*) appears unstained, with fibers of very variable sizes that do not clearly differentiate fiber types. (c) Regenerated muscle fibers of very heterogeneous size and morphology (asterisk), including spiral fibers (arrows) and splitting fibers (arrowheads). (d) Regenerated muscle fibers with central nuclei of abnormal size and morphology (asterisk); arrowheads indicate splitting fibers and arrow a ring fiber. Inset: The striated pattern is evident in the periphery of the muscle fiber. Original magnification: a, 5x; b, 20x; c, 20x; d, 20x. (a) and (c) Hematoxylin-eosin; (b) NADH-tr; (d) anti-desmin.

Regenerative response of rat skeletal muscle to the implantation of a collagen-based bone graft substitute

Eur J Transl Myol 35 (4) 13574, 2025 doi: 10.4081/ejtm.2025.13574

implantation, in our case osteogenic differentiation is not generated in the abnormal regeneration process. Understanding the interrelationship and interdependence between soft tissues and the skeleton is not only essential for correctly assessing aging processes,³⁴ but also for eval-

uating the efficacy of different tissue reconstruction strategies.³⁵ We believe that the results obtained in this study confirm the importance of considering the impact that different biomaterials, used for regenerative purposes in other adjacent tissues and organs, have on tissue regen-

Table 1. Percentage of muscle fibers showing cytoarchitectural changes at 60 days.

	NC	RC	FC	SC
Fibers with internalized nuclei	–	29.1% (2)	51.4% (3)	29.4% (2)
Splitting fibers	–	3.79% (1)	3.13% (1)	13.3% (1)
Ring fibre	–	–	–	0.98% (1)
Whorled fibers	–	–	–	1.76% (1)

In brackets, each parameter was assigned a score 1 through 4 per microscopic field whereby grade 1 (<25%), grade 2, 26–50%; grade 3, 51–75%; grade 4, >76%; –, no detected.

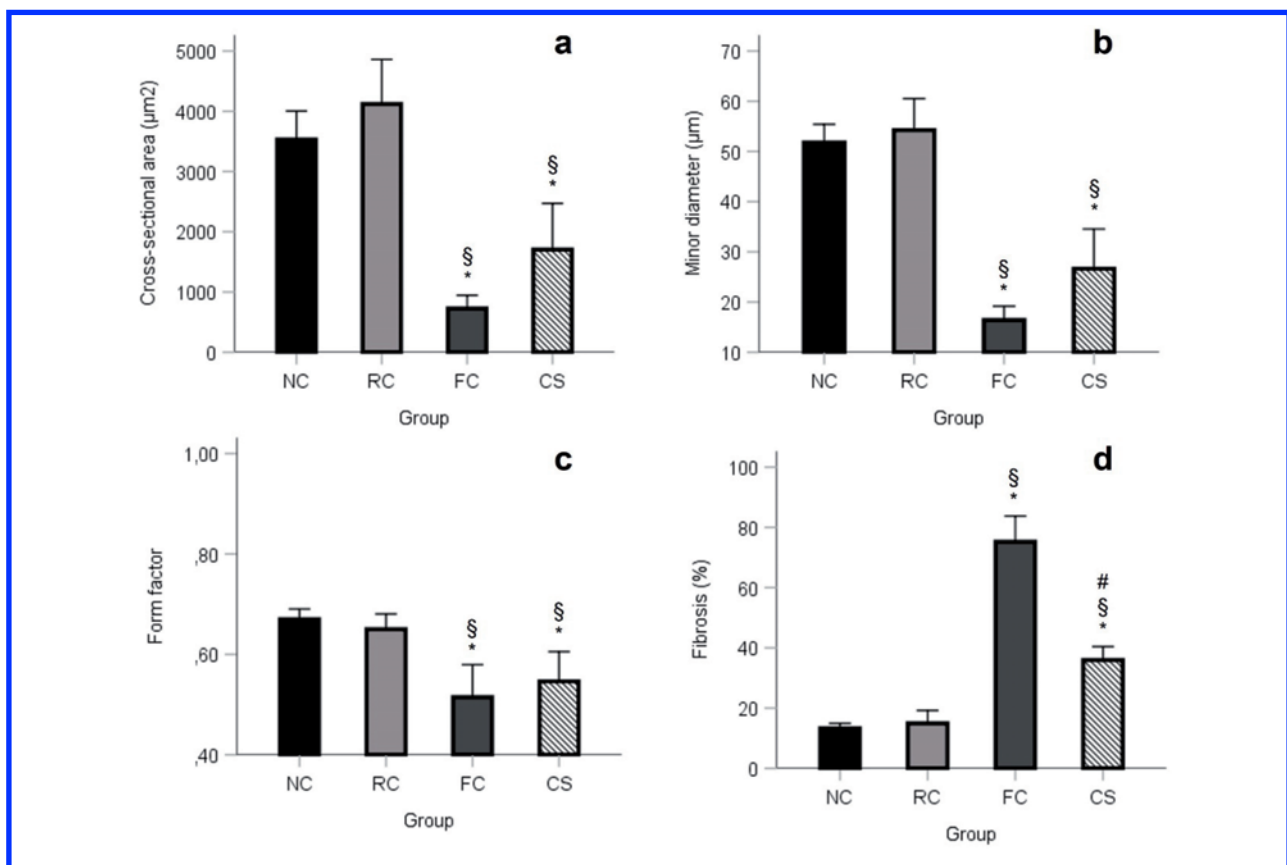


Figure 5. Bars represent the mean value of the morphometric parameters measured for each group. Error bars represent mean \pm 2 SEM (standard error of the mean). Significance was set at $p < 0,05$. (a) Myofiber cross-sectional area (μm^2). (b) Myofiber minor diameter (μm). (c) Form factor is a shape descriptor that estimates how similar a particle is to a perfect circle, ranging from 0 (absolute irregularity in shape) to 1 (a perfect circle). (d) The percentage of the area occupied with fibrous tissue is out of the total. *Significant differences $p < 0,05$ vs NC; §, significant differences $p < 0,05$ vs RC. #significant differences $p < 0,05$ vs FC.

Table 2. Histomorphometry parameters at 60 days.

	Cross-sectional area (μm^2)	Minor diameter (μm)	Form factor	Fibrosis (%)
NC	3529.86 \pm 237.11	51.77 \pm 1.82	0.67 \pm 0.01	13.26 \pm 0.82
RC	4119.54 \pm 370.57	54.23 \pm 3.15	0.65 \pm 0.02	14.92 \pm 2.14
FC	724.60 \pm 109.81 ^{§*}	16.41 \pm 1.38 ^{§*}	0.51 \pm 0.03 ^{§*}	75.19 \pm 4.29 ^{§*}
CS	1704.43 \pm 382.71 ^{§*}	26.63 \pm 3.96 ^{§*}	0.54 \pm 0.03 ^{§*}	35.93 \pm 4.6 ^{§*#}

Values are expressed as mean \pm SEM (standard error of mean). *Significance was set at $p < 0,05$ vs NC; [§], significant differences $p < 0,05$ vs RC; #, significant differences $p < 0,05$ vs FC.

erative capacity. In this sense, the observations and data from our work indicate that a material used for bone reconstruction hinders the correct evolution of regeneration that occurs in a muscle injury. In our opinion, this could be important when reconstructing a bone injury close to a muscle injury. Since our study was conducted in a mouse model, the potential translation of our results to humans must always be approached with caution. In any case, we thought it would be interesting to conduct this experiment in an animal model that combines volumetric muscle injury with bone injury, since both situations are combined in combat wounds and major trauma.

In our opinion, this study has some limitations. First, we did not include periods prior to 21 days, since, for comparative purposes, in a normal regenerative process (as in the RC group), muscle fibers are fully regenerated 20 days after the injury.¹⁰ This is a consequence of the fact that, in volumetric deficit injuries, the degenerative and inflammatory processes are prolonged over time.¹⁵ Since in our model, not only muscle fibers with significant cytoarchitectural abnormalities but also new intramuscular tendons were generated, it would be interesting to analyze previous periods to study the formation of new myotendinous junctions to determine whether these may also present histological abnormalities. We believe this question is of interest in the field of sports traumatology, since the myotendinous junction is the most frequent site of injury and re-injury.³⁶ These questions will be addressed in our laboratory in the near future.

Conclusions

Based on the present data, a collagen-based bone matrix substitute can be fully integrated into skeletal muscles following implantation in a volumetric defect. This biomaterial does not inhibit the inherent regenerative capacity of skeletal muscle, possibly due to its porous nature. However, it interferes with regenerative muscle fibers' normal growth and development by promoting the fibrotic aspect of the regenerative response. The identification of large intramuscular tendons points towards a potential role for this bone matrix substitute in tendon reconstruction strategies that is yet to be explored.

List of abbreviations

NC, normal control group
RC, regenerative control group
FC, fibrotic control group
CS, collagen scaffold group

Acknowledgments

The authors are grateful to Mr. Antonio Agüera for all technical support and assistance.

Funding

This research received no external funding.

Conflict of interest

The authors declare no competing interests

Ethics approval

The study was approved by the General Directorate of Agricultural and Livestock Production of the Junta de Andalucía (Ref. 07/09/2017/121), the Ethics Committee for Animal Experimentation at the University of Cordoba (Ref. 2017IP/05).

Contributions

Conceptualization:FL-C, JP-A; methodology: FLC, MJG-B, MAP-T, IJ; formal analysis: FL-C, MJG-B; investigation: MJG-B, MAP-T, IJ; supervision: RV, JP-A; Writing original draft: FL-C, MJG-B, RV, JP-A; writing revision and editing: FLC, MJG-B, JP-A. All authors read and approved the final edited manuscript.

Availability of data and materials

All data generated or analyzed during this study are included in this published article.

Corresponding author

José Peña-Amaro. Research Group in Muscle Regeneration. Department of Morphological and Sociosanitary Sciences, Faculty of Medicine and Nursing, University of Cordoba, Av. Menedez Pidal s/. 14004. Cordoba, Spain. Telephone (+34) 957 218 264. Fax: (+34) 957 218 246. ORCID ID: 0000-0002-2637-1112
E-mail: cm1peamj@uco.es

Co-authors

Fernando Leiva-Cepas
ORCID ID: 0000-0002-0014-3816
E-mail: fleivacepas@gmail.com

Maria Jesús Gil-Belmonte
ORCID ID: 0000-0002-1088-6576
E-mail: mjgilbelmonte@gmail.com

Ignacio Jimena
ORCID ID: 0000-0002-5095-6962
E-mail: cm1jimei@uco.es

Maria Angeles Peña-Toledo
ORCID ID: 0000-0002-9388-5893
E-mail: angelespe87@gmail.com

Rafael Villalba Montoro
ORCID ID: 0000-0001-5600-3276
E-mail: rafael.villalba.sspa@juntadeandalucia.es

References

1. Turner NJ, Badylak SF. Regeneration of skeletal muscle. *Cell Tissue Res* 2012;347:759-74.
2. Edouard P, Reurink G, Mackey AL, et al. Traumatic muscle injury. *Nat Rev Dis Primers* 2023;9:56.
3. Sicari BM, Dearth CL, Badylak SF. Tissue engineering and regenerative medicine approaches to enhance the functional response to skeletal muscle injury. *Anat Rec (Hoboken)* 2014;297:51-64.
4. Forcina L, Cosentino M, Musarò A. Mechanisms regulating muscle regeneration: insights into the inter-related and time-dependent phases of tissue healing. *Cells* 2020;9:1297.
5. Raghuram A, Singh A, Chang DK, et al. Bone grafts, bone substitutes, and orthobiologics: applications in plastic surgery. *Semin Plast Surg* 2019;33:190-99.
6. Testa S, Fornetti E, Fuoco C, et al. The war after war: volumetric muscle loss incidence, implication, current therapies and emerging reconstructive strategies, a comprehensive review. *Biomedicines* 2021;9:564.
7. Kunert-Keil C, Botzenhart U, Gedrange T, Gredes T. Interrelationship between bone substitution materials and skeletal muscle tissue. *Ann Anat* 2015;199:73-8.
8. Pradel W, Lauer G. Tissue-engineered bone grafts for osteoplasty in patients with cleft alveolus. *Ann Anat* 2012;194:545-8.
9. Leiva-Cepas F, Benito-Ysamat A, Jimena I, et al. Ultrasound and histological correlation after experimental reconstruction of a volumetric muscle loss injury with adipose tissue. *Int J Mol Sci* 2021;22:6689.
10. Jiménez-Díaz F, Jimena I, Luque E, et al. Experimental muscle injury: correlation between ultrasound and histological findings. *Muscle Nerve* 2012;45:705-12.
11. Leiva-Cepas F, Jimena I, Ruz-Caracuel I, et al. Histology of skeletal muscle reconstructed by means of the implantation of autologous adipose tissue: an experimental study. *Histol Histopathol* 2020;35:457-74.
12. Dubowitz VA, Sewry C, Oldfors A. *Muscle biopsy: A practical approach*. 5th Edition. Elsevier; 2021.
13. Schindelin J, Arganda-Carreras I, Frise E, et al. Fiji: an open-source platform for biological-image analysis. *Nat Methods* 2012;9:676-82.
14. Turner NJ, Pezzone MA, Brown BN, Badylak SF. Quantitative multispectral imaging of Herovici's polychrome for the assessment of collagen content and tissue remodelling. *J Tissue Eng Regen Med* 2013;7:139-48.
15. Aguilar CA, Greising SM, Watts A, et al. Multiscale analysis of a regenerative therapy for treatment of volumetric muscle loss injury. *Cell Death Discov* 2018;4:33.
16. Kin S, Hagiwara A, Nakase Y, et al. Regeneration of skeletal muscle using in situ tissue engineering on an acellular collagen sponge scaffold in a rabbit model. *ASAIO J* 2007;53:506-13.
17. Liu X, Gao Y, Long X, et al. Type I collagen promotes the migration and myogenic differentiation of C2C12 myoblasts via the release of interleukin-6 mediated by FAK/NF- κ B p65 activation. *Food Funct* 2020;11:328-38.
18. Grefte S, Kuijpers-Jagtman AM, Torensma R, Von den Hoff JW. Model for muscle regeneration around fibrotic lesions in recurrent strain injuries. *Med Sci Sports Exerc* 2010;42:813-9.
19. De Paolis F, Testa S, Guarnaccia G, et al. Long-term longitudinal study on swine VML model. *Biol Direct* 2023;18:42.
20. Alexakis C, Partridge T, Bou-Gharios G. Implication of the satellite cell in dystrophic muscle fibrosis: a self-perpetuating mechanism of collagen overproduction. *Am J Physiol Cell Physiol* 2007;293:C661-9.
21. Grefte S, Adjobo-Hermans MJW, Versteeg EMM, et al. Impaired primary mouse myotube formation on crosslinked type I collagen films is enhanced by laminin and entactin. *Acta Biomater* 2016;30:265-76.
22. Eugenis I, Wu D, Rando TA. Cells, scaffolds, and bioactive factors: Engineering strategies for improving regeneration following volumetric muscle loss. *Biomaterials* 2021;278:121173.
23. Kozan NG, Joshi M, Sicherer ST, Grasman JM. Porous biomaterial scaffolds for skeletal muscle tissue engineering. *Front Bioeng Biotechnol* 2023;11:1245897.
24. Kim J, Kasukonis B, Roberts K, et al. Graft alignment impacts the regenerative response of skeletal muscle after volumetric muscle loss in a rat model. *Acta Biomater* 2020;105:191-202.

Regenerative response of rat skeletal muscle to the implantation of a collagen-based bone graft substitute

Eur J Transl Myol 35 (4) 13574, 2025 doi: 10.4081/ejtm.2025.13574

25. Lee AS, Anderson JE, Joya JE, et al. Aged skeletal muscle retains the ability to fully regenerate functional architecture. *Bioarchitecture* 2013;3:25-37.
26. Hardy D, Besnard A, Latil M, et al. Comparative study of injury models for studying muscle regeneration in mice. *PLoS One* 2016;11:e0147198.
27. Peña J, Luque E, Noguera F, et al. Experimental induction of ring fibers in regenerating skeletal muscle. *Pathol Res Pract* 2001;197:21-7.
28. Pontén E, Fridén J. Immobilization of the rabbit tibialis anterior muscle in a lengthened position causes addition of sarcomeres in series and extra-cellular matrix proliferation. *J Biomech* 2008;41:1801-4.
29. Csapo R, Gumpenberger M, Wessner B. Skeletal muscle extracellular matrix - what do we know about its composition, regulation, and physiological roles? A Narrative Review. *Front Physiol* 2020;11:253.
30. Winkler T, von Roth P, Matziolis G, et al. Time course of skeletal muscle regeneration after severe trauma. *Acta Orthop* 2011;82:102-11.
31. Swery CA, Goebel HH. General pathology of muscle disease. In: Goebel HH, Swery CA, Weller RO, eds. *Muscle Disease: Pathology and Genetics*, second edition. John Wiley & Sons Ltd; 2013. pp 19-38.
32. Roßbach BP, Gülecüyüz MF, Kempfert L, et al. Rotator cuff repair with autologous tenocytes and biodegradable collagen scaffold: a histological and biomechanical study in sheep. *Am J Sports Med* 2020;48:450-59.
33. Davies OG, Liu Y, Player DJ, et al. Defining the balance between regeneration and pathological ossification in skeletal muscle following traumatic injury. *Front Physiol* 2017;8:194.
34. Scarano A, Ceccarelli M, Marchetti M, et al. Soft tissue augmentation with autologous platelet gel and β -TCP: a histologic and histometric study in mice. *Biomed Res Int* 2016;2016:2078104.
35. Marchetti E, Mancini L, Bernardi S, et al. Evaluation of different autologous platelet concentrate biomaterials: morphological and biological comparisons and considerations. *Materials (Basel)* 2020;13:2282.
36. Pedret C, Peña-Amaro J, Balius R, Järvinen T. Histological definition of skeletal muscle injury: a guide to nomenclature along the connective tissue sheath/structure. *Sports Med* 2025;55:1061-5.

Disclaimer

All claims expressed in this article are solely those of the authors and do not necessarily represent those of their affiliated organizations, or those of the publisher, the editors and the reviewers. Any product that may be evaluated in this article or claim that may be made by its manufacturer is not guaranteed or endorsed by the publisher.

Submitted: 1 January 2025.

Accepted: 30 May 2025.

Early access: 22 July 2025.

Online supplementary material:

Supplementary Figure 1. (a) Volumetric defect in the tibialis anterior muscle, (b) bone substitution material, (c) collagen matrix implant within the volumetric defect.

Supplementary Figure 2. CS group. Sixty days postimplantation. (a) The image shows a large tendon (asterisk) in the vicinity, of which there is significant fascicular atrophy (lower left) compared to the normal muscle fibers on the right. (b) Inset of the image (a) with significant perimysial fibrosis separating the atrophic muscle fascicles. (c) Fascicular atrophy and poor fiber-type differentiation. Original magnification: a, 10x; b, 40x; c, 20x. (a) and (b), Masson's trichrome; (c), NADH-tr.

Supplementary Figure 3. (a) NC group 60 days postimplantation, (b) RC group 60 days postimplantation, (c) FC group 60 days postimplantation, (d) CS group. 60 days postimplantation. In NC, a higher percentage of type III collagen is observed. In RC, the percentage of collagen I and II is balanced. In FC and CS, type I collagen is clearly predominant. Original magnification: 10x. Herovici's polychrome staining.